The Effect of Noise and Diversity on Synthetic Array Radar Imagery

S. Butman and R. G. Lipes
Communications Systems Research Section

This article investigates synthetic aperture radar (SAR) image quality as a function of received signal-to-noise ratio, multiple looks or diversity averaging of "speckle," contrast, and resolution. Theoretical and simulation results are presented. The data are useful for tradeoff analyses in the design of the SAR, the image processing system, and the telemetry system. Photographs have been made to show the effect of the above-mentioned parameters. The general conclusion is that diversity averaging produces an image far superior to that obtained via equivalent receiver signal-to-noise improvement.

I. Introduction

One aspect of the DSN Advanced Systems Program is investigation of the flight–ground–mission control interfaces. This has the salutary feature of resource savings to NASA through optimum (in the sense of multimission support cost) flight and ground system design. A good example is the standard command detector breadboard development. Other tradeoff areas are also being examined including, in the near term, operational problems, and in the longer term, a look at likely flight projects which will require higher link performance and instrumentation.

A Venus-Orbiting Imaging Radar (VOIR) mapper has been proposed for the 1980's. The likelihood for such a mission is high, particularly since a similar Earth-orbiting mission, Sea Satellite (SEASAT), has been approved. When a VOIR-type mission is approved it will require a link capability up to 20 dB better than the current Mariner Jupiter-Saturn spacecraft/64-m antenna combination can provide at X-band. Furthermore, once such a high rate link (5–25 megabits/s) comes into being, it will be necessary to equip the Network with appropriate instrumentation to receive, detect, decode, and handle these data. These science data can be anticipated to be essentially raw radar echoes received on the spacecraft and telemetered to Earth, either in real-time or after temporary storage on board. These raw data will require processing into an image either at a DSN station or at the mission communication and control center, depending on processing cost vs ground communication cost. In either case, the DSN will need a capability to meet certain performance criteria pertaining to data quality (in this case, synthetic array radar image quality).

The purpose of this paper is to report some progress on the relationship between image quality, signal-to-noise ratio, and processing techniques. This type of information is expected, ultimately, to influence the design of the spacecraft and the ground system. Here we will be discussing picture formation via synthetic array radar signal processing. Pictures obtained in this manner exhibit "speckle" or self-noise, which can be removed through the introduction of diversity. We first give a brief theoretical discussion of the underlying causes of speckle and its removal, followed by a discussion of simulation results and conclusions on this phase of the study.

II. Speckle

When monochromatic coherent radiation is scattered off a surface, the return is a coherent superposition of contributions from the elementary scattering centers of the surface. When the roughness or height variation of the surface is approximately equal to or greater than the wavelength of the radiation,[1] the phases of the contributions from the elementary scattering centers can be closely approximated as independent random variables uniformly distributed between 0 and 2π. When the number of scattering centers is sufficiently large so that the central limit theorem can be applied to the superposition of elementary contributions, the amplitude of the return signal can be closely approximated as a Rayleigh distributed random variable.[2] The power s of the return will be exponentially distributed, having the probability density function

$$P(s) = e^{-s/S}\frac{1}{S} \qquad (1)$$

where S is the mean power of the return. This phenomenon has recently been called "speckle" by the workers in optics (Refs. 2–4), although it has been noted by the workers in radar (Ref. 5) and certainly dates back to Lord Rayleigh (Ref. 6).

In many cases we want to obtain information about the features of the illuminated surface from the return signal. However, the features of a certain area are related to the mean power S of the return from this area, while the actual power s of the return is probabilistic. For this reason we need to employ some form of diversity reception to obtain the average power. Typically, this diversity takes the form of space diversity, which means that the surface is observed from independent vantage points and the results of the independent "multiple looks" are averaged. Another common form is frequency diversity, in which results from independent looks with radiation of different frequencies are averaged. Whatever the form, the results from multiple looks must be added incoherently to approximate the average power return from the surface.

III. Speckle Reduction via Multiple Looks

In this study we wanted to simulate the effects of the "speckle" phenomenon as it would apply to a picture processed from satellite radar data. We chose an Earth Resources Technology Satellite (ERTS) optical picture that was put on magnetic tape with picture elements (pixels) representing 57- × 79-m resolution cells. The picture shown in Fig. 1 (low contrast original) represents the ERTS data from an area approximately 15.4 km left-right by 21.3 km up-down (270 × 270 pixels). Each pixel is quantized to 6 bits on the tape, representing 1 of 64 shades between black and white. To simulate the radar "speckle" we replaced each pixel value with a random variable exponentially distributed according to Eq. (1), with the mean value S taken as the original pixel value. This resulted in the picture (low contrast, 1 look) shown in the lower center of Fig. 1. As one can see, the image content is almost entirely lost. This photograph represents an extreme effect that the radar speckle would have on a single "look."

We then repeated this procedure 4, 16, and 64 times, and averaged the independent results to generate the pictures (low contrast series) shown in the center region of Fig. 1. Mathematically, we generated N identically distributed random variables, $s_1,\cdots,s_M$ and computed and plotted

$$s_M = \frac{1}{M}\sum_{i=1}^{M} s_i \qquad M = 1,4,16,64$$

for each pixel. Here, M represents the number of "looks."

[1]This admittedly crude definition of a "rough" surface is qualitatively the Rayleigh criterion, which states that a surface is rough or smooth depending on whether the height variation at grazing angle is respectively greater than or less than $\lambda/8 \sin\gamma$, λ being the wavelength of the radiation. For a discussion of the validity of the Rayleigh criterion, see Ref. 1.

[2]The theoretical hypotheses under which the amplitude will be Rayleigh-distributed are enumerated in Ref. 1, Chapter 7. Published data that verify the validity of these hypotheses are surprisingly rare; in fact, we have been unable to find any data of terrestrial radar returns that directly exhibit a Rayleigh amplitude distribution. Reference 1, page 463, presents evidence for the lunar radar return with a Rayleigh-distributed amplitude. Reference 5, pages 515–518, gives experimental evidence of Rayleigh-distributed amplitudes in radar returns from the sea.

The mean of s_M is still S, but the variance

$$\sigma_M^2 = \overline{(s_M - S)^2} = \frac{S^2}{M} \tag{2}$$

is reduced by the factor $1/M$ compared to a single look. Therefore, the signal-to-noise ratio (SNR) per pixel as defined by ratio of power in signal to standard deviation of that power

$$SNR_{pixel} = \frac{S}{\sigma_M} = \sqrt{M} \tag{3}$$

increases 3 dB per 4-fold increase in M. From these photographs we see that a reasonable facsimile of the original picture is obtained for some number of looks between 16 and 64.

The original Earth Resources Technology Satellite (ERTS) picture and the pictures simulating the multiple looks are all of a scene with rather low contrast. Figure 2 shows a histogram of the original pixels in the scene. The ordinate is the number of pixels n_s having a given value S (between 0 and 63), and the abscissa is the value S. Even though 64 contrast levels are available, these pictures are effectively using only about 10 levels. To increase contrast in the developed original image we uniformly "stretched" the pixel values to cover the full dynamic range of 64 levels by rescaling the data on the tape. This was accomplished for each pixel by the mapping,

$$S \rightarrow S' = 13(S - 10)/3 \tag{4}$$

where S' is the new pixel value given the cell that originally had pixel value S. (Of course, new pixel values less than 0 or greater than 63 were set to 0 and 63, respectively.) The high-contrast ERTS picture now has the histogram shown in Fig. 3. This higher-contrast original was once again studied for the effects of speckle. The resulting ERTS picture and those simulating 1, 4, 16, and 64 looks (high contrast series) are shown in the left-hand column of Fig. 1. Higher original contrast considerably improves the speckled image. In fact, the 16-look simulation reveals most of the features of the original high-contrast ERTS picture.

IV. Resolution vs Multiple-Look Tradeoff

Next, we studied the procedure of sacrificing resolution to increase the effective number of looks. This was accomplished by averaging returns from adjacent resolution cells. We took the multiple-look pictures of the center column of Fig. 1 (low contrast series) and replaced the pixel values of 4 adjacent pixels (2 up-down and 2 left-right) by the average of the 4. This procedure is illustrated in Fig. 4. Notice that the effective resolution cell area has increased by a factor of 4 as the result of this averaging, so we have sacrificed resolution to obtain more looks. Since we have increased the effective number of looks by a factor of 4, the information content of the low-resolution M look system should be close to that of the original $4M$-look system. The problem in making a visual comparison is that the resolution limit of the original system is determined by the area of a single pixel, while for the low-resolution system, it is determined by the area of 4 adjacent pixels. To facilitate this comparison we have decreased the area of the low-resolution series by a factor of 4. In Fig. 1 we see the resolution vs multiple-look tradeoff by comparing the center and right-hand columns. The information content of low-resolution M-look system is greater than that of the original M-look system and approaches but does not reach that of the original $4M$-look system for $M = 1$, 4, and 16.

V. Effect of Additive Noise

To investigate the effects of receiver and downlink noise on picture quality, we introduced varying amounts of additive white Gaussian noise (AWGN) to the multi-look pictures. Since each pixel is formed by envelope-detecting an in-phase and a quadrature signal, which are themselves contaminated by receiver noise, the situation is described by

$$\begin{aligned} v_I &= a_I + n_I \\ v_Q &= a_Q + n_Q \end{aligned} \tag{5}$$

where a_I, a_Q are the in-phase and quadrature voltages in the pixel from the scene in the absence of noise, and n_I, n_Q are the corresponding contaminating voltages in the pixel due to noise. The signal power s, noise power n, and total power v in the pixel are given by

$$\begin{aligned} s &= a_I^2 + a_Q^2 \\ n &= n_I^2 + n_Q^2 \end{aligned} \tag{6}$$

and

$$v = (a_I + n_I)^2 + (a_Q + n_Q)^2$$

These random variables are exponentially distributed since they are sums of squares of pairs of independent, identically distributed, zero mean gaussian random

variables. Moreover, since a_I, a_Q, n_I and n_Q are all statistically independent,

$$\overline{s} = \overline{a_I^2 + a_Q^2} = S$$
$$\overline{n} = \overline{n_I^2 + n_Q^2} = N \tag{7}$$

and

$$\overline{v} = S + N = V$$

Consequently,

$$p(v) = \frac{1}{V} e^{-v/V} \tag{8}$$

and we can produce the effect of noise by generating exponentially distributed pixels with parameter $S+N$, where S depends on the value of the original pixel and N is determined by the amount of noise we wish to introduce. This receiver signal-to-noise ratio is then

$$SNR = \frac{S}{N} \tag{9}$$

The pixel SNR will now be given by

$$SNR_{pixel} = \frac{S}{\sqrt{\overline{(v_M - V)^2}}} \tag{10}$$

where v_M is the M look average of the noisy observables $v_1, v_2, \cdots, v_M$, i.e., $v_M = \frac{1}{M} \sum_{i=1}^{M} v_i$. Using Eq. (2) we see this can be expressed as

$$SNR_{pixel} = \sqrt{M} \frac{S}{S+N} \tag{11}$$

which reduces to the "noiseless" case (3) as it should when $N = 0$. We chose values of N, the average noise power, to be 25, 12.5, 6.25, 2.5, and 0.79, corresponding roughly to receiver SNRs of 0, 3,6, 10, and 15 dB, respectively, since, as can be seen from Fig. 2, the average pixel intensity over the picture is close to 25. We replaced each pixel value S with the random variable v distributed according to Eq. (8) with $V = S+N$ from which N was subtracted. This subtraction was performed so that the nonlinearity imposed by the 6-bit quantization would not introduce unnecessary distortion by exceeding the dynamic range. The results for 0-, 3-, 6-, 10-, and 15-dB receiver SNR are shown respectively in Fig. 5 for M look systems where $M = 1,4, 16$, and 64. As one can see, increasing receiver SNR improves picture quality but not nearly as dramatically as increasing the number of looks. We can gain a rough understanding of the relationship between picture quality, number of looks, and receiver SNR by considering a typical pixel SNR. Admittedly, a single number such as pixel SNR cannot represent an entire picture, but it is commonly used to provide a rough index of picture quality. The mean power from the ith cell is $S_i + N$, but the "signal" portion of this return is S_i. The standard deviation of the power in an M-look system is $M^{-1/2}(S_i + N)$, so the pixel SNR is

$$SNR_{pixel} = \frac{\sqrt{M}\, S_i}{(S_i + N)} = \frac{\sqrt{M}}{(1 + 1/SNR_i)} \tag{12}$$

To obtain some feeling for the relation, consider an M-look system with infinite receiver SNR. A typical pixel SNR is $\sqrt{M}$. Now consider a system with $4M$ looks. This system will be better in terms of pixel SNR than the original zero receiver noise M-look system so long as its receiver SNR is greater than 1. We see that this result is borne out by comparing the M-look pictures of 10 and 15 dB with the $4M$-look pictures of 0 dB. We see that the $4M$-look pictures of 0 dB are better in each case shown ($M = 1$, 4, and 16). Also, from Eq. (12) and the pictures of Fig. 5 we see that receiver SNRs greater than 10 dB do little to enhance picture quality.

VI. Conclusions and Discussion of Results

In this study we have presented our results by demonstrating photographs of varying numbers of looks, contrast, resolution, and receiver SNR to be compared visually with original photographs of high and low contrast, fixed resolution, and infinite receiver SNR. We have seen qualitatively that with large receiver SNR, 64 looks in the low-contrast case, and perhaps as few as 16 looks in the high-contrast case provide a picture that certainly contains the salient features of the original. Of course, the fidelity required of the multilook image and the comcomitant criteria to measure this fidelity determine the actual number of looks and receiver SNR which the system must have. This in turn determines the coverage, resolution, and telemetry data rate of the overall system.

References

1. Beckman and Spizzichino, *The Scattering of Electromagnetic Waves from Rough Surfaces*, MacMillan Co., New York, 1963.
2. Schiffner, G., *Proc. IEEE*, 53, 1245, 1965.
3. Gabor, D., *IBM J. Theo. Develop.*, 14, 509, 1970.
4. Enloe, L., *Bell Sys. Tech. J.*, 46, 1479, 1967.
5. MIT Radiation Laboratory Series, Vol. 13, edited by D. E. Kerr.
6. Lord Rayleigh, *The Theory of Sound*, MacMillan Co., 3rd Edition, London, 1896.

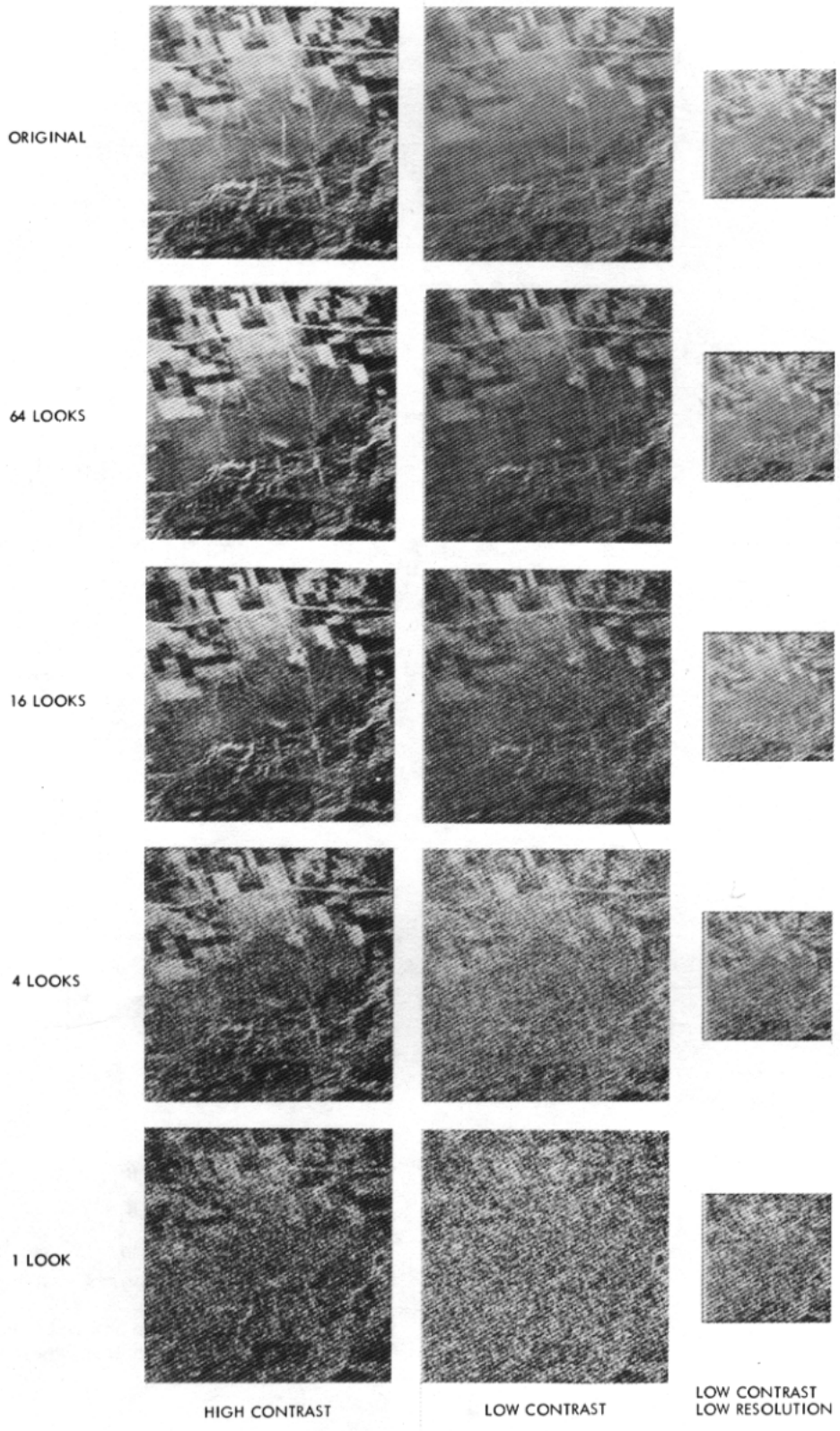

Fig. 1. Original ERTS photograph and photographs showing effects of 1, 4, 16, and 64 looks for high-contrast, low-contrast and for low-contrast, low-resolution series

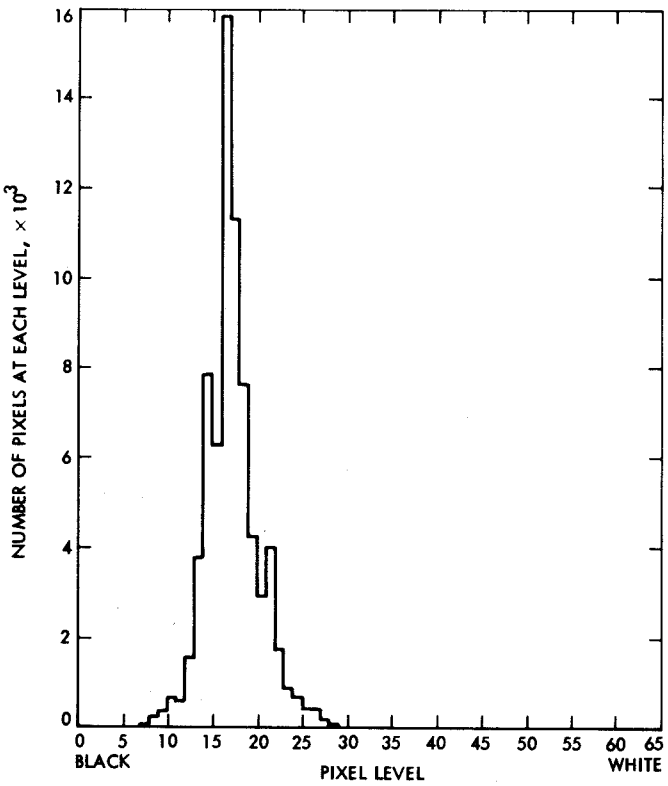

Fig. 2. Histogram for low-contrast ERTS original showing number of pixels having a value S vs the value S_n (S = 0, • • • , 63)

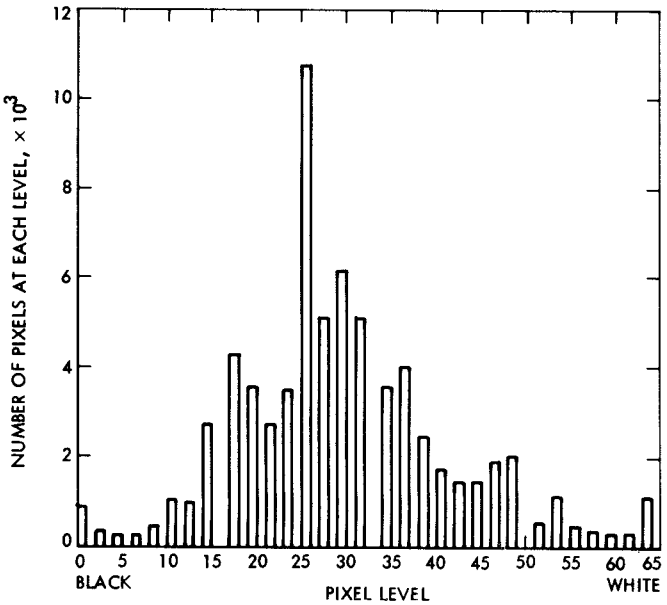

Fig. 3. Histogram for high-contrast original showing number of pixels having a value S vs the value S (S = 0, • • • , 63)

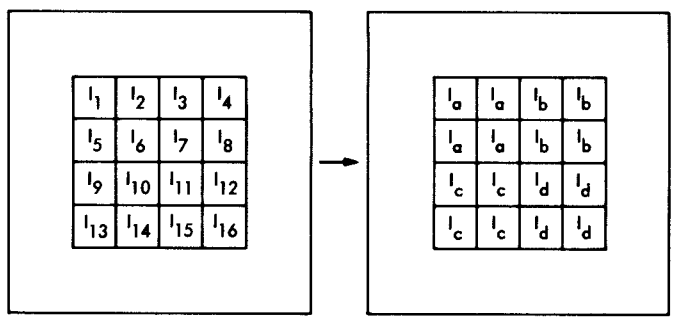

$$I_a = 1/4\,(I_1 + I_2 + I_5 + I_6)$$
$$I_b = 1/4\,(I_3 + I_4 + I_7 + I_8)$$
$$I_c = 1/4\,(I_9 + I_{10} + I_{13} + I_{14})$$
$$I_d = 1/4\,(I_{11} + I_{12} + I_{15} + I_{16})$$

Fig. 4. Diagram illustrating how resolution cell averaging was performed for low-contrast, low-resolution series

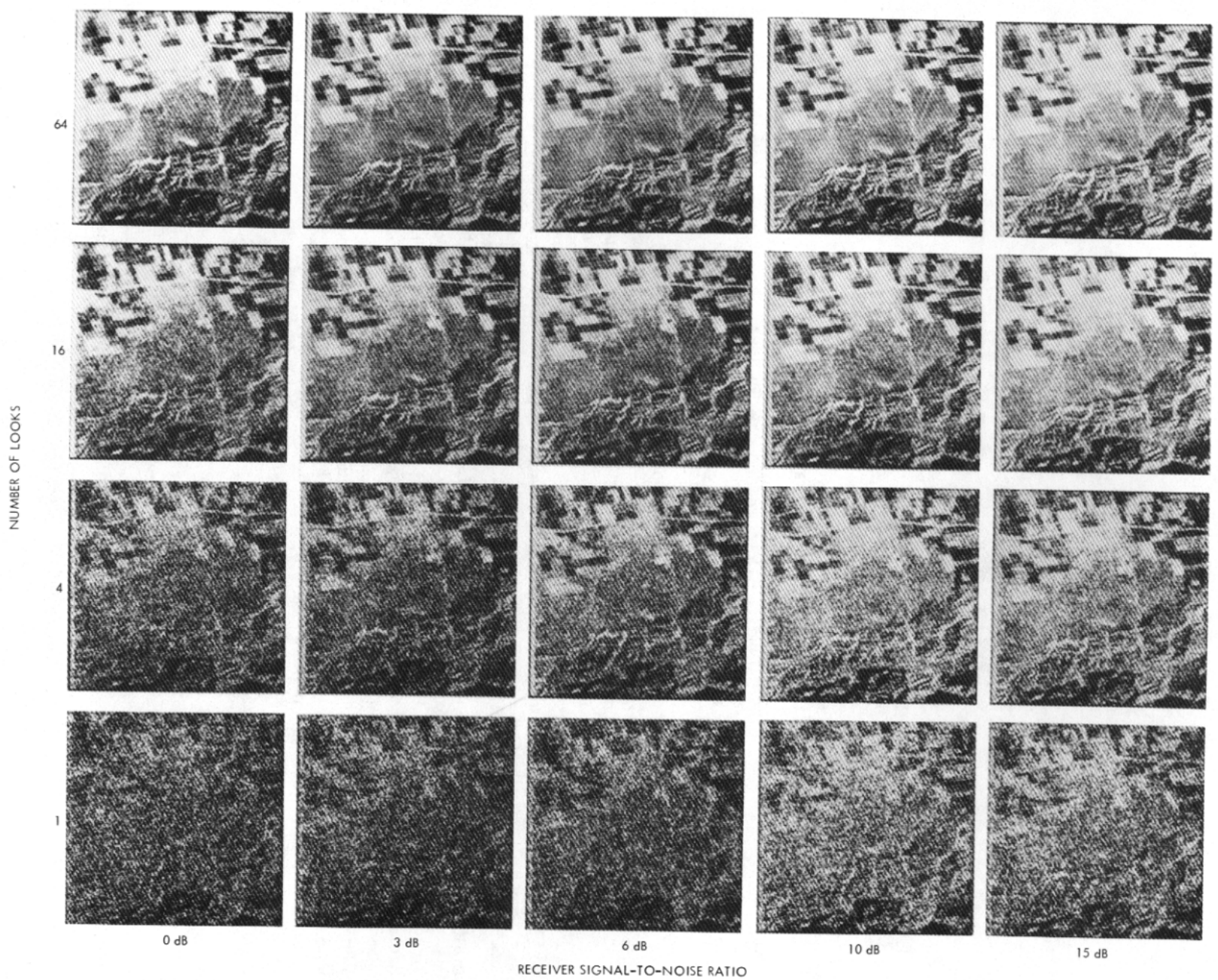

Fig. 5. High-contrast photographs illustrating effects of varying number of looks (M = 1,4,16, and 64) and varying receiver signal-to-noise ratio (SNR = 0,3,6,10, and 15 dB) on simulated SAR image quality